



ELSEVIER

Journal of Crystal Growth 225 (2001) 440–444

JOURNAL OF
**CRYSTAL
GROWTH**

www.elsevier.nl/locate/jcrysgr

Defect segregation in CdGeAs₂

Peter G. Schunemann^{a,*}, Scott D. Setzler^a, Thomas M. Pollak^a, Aaron J. Ptak^b,
Thomas H. Myers^b

^a Sanders, A Lockheed Martin Company, MER15-1813, P.O. Box 868, Nashua, NH 03061-0868, USA

^b Department of Physics, West Virginia University, Morgantown, WV 26506, USA

Abstract

Increased axial temperature gradients and growth rates have resulted in segregation of unwanted absorbing defects to the edges of CdGeAs₂ single crystals produced by the horizontal gradient freeze technique. Long-wavelength infrared imaging of polished boules revealed a “clear” central core with absorption losses 26 times lower than in the darker edge regions. This pronounced segregation is attributed to the preferred incorporation of native defects at facets that form near the side walls of the horizontal boat. EPR, GDMS, and Hall effect analysis were used to characterize the nature of these defects. © 2001 Elsevier Science B.V. All rights reserved.

Keywords: A1. Directional solidification; A1. Segregation; A1. Point defects; A2. Gradient freeze technique; B1. Chalcopyrites; B2. Nonlinear optical materials

1. Introduction

Despite having one of the highest nonlinear optical coefficients among known compounds (236 pm/V), severe cracking and excessive defect-related absorption losses have historically limited the usefulness of CdGeAs₂ for frequency-shifting lasers in the mid-infrared spectral range [1,2]. Horizontal gradient freeze growth in two-zone transparent furnaces has now been established as a high-yield process for producing crack-free, single crystal CdGeAs₂ [3–5], and isolated samples have exhibited the low absorption losses required for efficient device operation [6,7].

Unfortunately, the absorption losses varied substantially (by an order of magnitude or more) in samples cut from different boules and even among samples cut from the same boule. Spectrophotometer measurements indicated that boules generally exhibited the highest transmission near the center (radially) and at the first-to-freeze end, but even these observations were erratic. Because of its narrow band gap, CdGeAs₂ could not be inspected with a transmission infrared microscope or even a hand-held IR viewer, techniques that greatly benefited the development of related chalcopyrite semiconductors ZnGeP₂ and Ag-GaSe₂. Hence it was unclear whether the variations in transmission arose from internal cracks or scattering centers (such as inclusions, voids or precipitates) or from an actual non-uniform distribution of absorbing defects.

Here we report the use of a unique long-wave infrared (LWIR) imaging system which allows

*Corresponding author. Tel.: +1-603-885-5041; fax: +1-603-885-0207.

E-mail address: peter.g.schunemann@lmco.com (P.G. Schunemann).

polished CdGeAs₂ boules to be viewed in transmission for the purpose of mapping internal macroscopic defects. This technique revealed distinct “light” and “dark” regions corresponding to areas of high and low transmission, respectively, at the 8- μm peak sensitivity wavelength of the camera. The contrast between these regions, as well as their morphology, was dependent on the crystal growth parameters and the thermal environment of the horizontal transparent furnace. These conditions can be optimized to force the undesirable dark regions to the edges of the “D-shaped” horizontal boule which are removed during processing, leaving behind a central core from which low-loss device crystals can be fabricated.

2. Long-wavelength infrared imaging

The LWIR imaging system used in this work was constructed at Sanders, a Lockheed Martin Company [8]. The system is based on a scanning HgCdTe focal plane array operating at ~ 60 K with a peak sensitivity at a wavelength of ~ 8 μm . A 50 K black-body source provided uniform background illumination of boules with ground and polished flats on the top and bottom surfaces.

Fig. 1 shows a LWIR image of a 19-mm-diameter, 140-mm-long CdGeAs₂ boule grown by the HGF technique. (The growth process used is described in detail in [3–5]. This crystal was grown in a PBN boat from a stoichiometric melt at a rate of 0.5 mm/h with an axial gradient of 2°C/cm under an overpressure of ~ 1 atm argon to suppress vaporization of Cd and As. Growth was along the

c -axis as shown, with the a -axis normal to the top surface.) The image illustrates a dramatic radial inhomogeneity in the infrared transmission: a relatively clear central core runs along the full length of the crystal, surrounded by highly absorbing dark regions along both sides of the horizontal boule. Fig. 2a shows the image through a cross-sectional slice, indicating angled, well-defined boundaries separating the dark and light regions.

Growth at lower axial gradients and growth rates (1–1.5°C/cm, 0.25 mm/h) reduced the contrast between these two regions, resulting in more homogeneous material. Unfortunately the absorption coefficient in the central region increased substantially to an intermediate value between those measured in the light and dark areas, respectively. Directional solidification at higher axial gradients (~ 5 °C/cm), however, resulted in even more pronounced segregation, as shown in Fig. 2b. Note that the clear central core is widened, and the boundaries are sharper and oriented at 45° with respect to the horizontal a -axis diameter. The sharpness of these boundaries, the high contrast

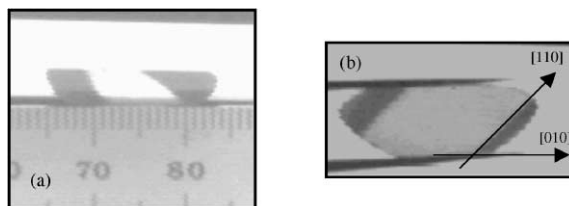


Fig. 2. Cross-sectional LWIR view of CdGeAs₂ crystals grown along [00 1] with axial temperature gradients of (a) 2°C/cm and (b) 5°C/cm.

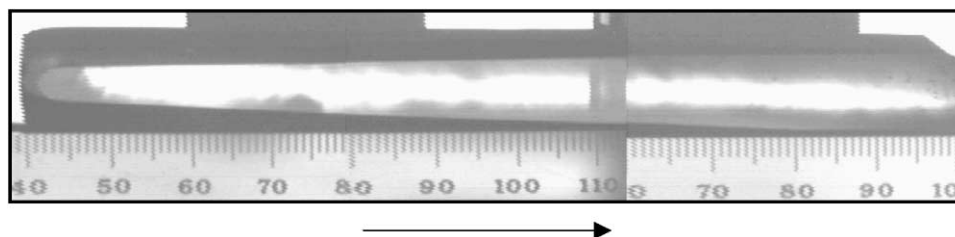


Fig. 1. LWIR image of a polished CdGeAs₂ crystal grown by the HGF technique (arrow indicates [00 1] growth direction).

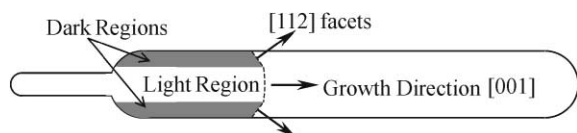


Fig. 3. Faceted growth mechanism responsible for radial segregation of absorbing defects in CdGeAs₂.

between the two regions, and the absence of any visible precipitates, inclusions, or cracks, confirms that the source of CdGeAs₂'s non-uniform optical properties is based on differences in absorption rather than scattering.

The inhomogeneous absorption described above appears to arise from the preferred segregation of absorbing defects toward the edges of the boule. Facet growth is proposed as the mechanism for the observed segregation behavior, as illustrated in Fig. 3. Observation of the CdGeAs₂ solid–liquid interface during HGF growth (a possibility unique to transparent furnaces) indicates that it is flat or slightly convex across most of the boule diameter, but close inspection of the region near the side walls of the boat revealed the presence of tiny 45° facets. It has long been established that facet growth leads to “core” formation, resulting in an inhomogeneous distribution of impurities in other semiconductors such as Ge and InSb [9,10]. InSb crystals pulled from a melt exhibited higher donor concentrations (up to 15 ×) on macroscopic (111) facets compared to off-facet growth [10]. The 45° angles of the observed facets relative to the *c*-axis growth direction, combined with the 45° boundary (relative to the *a*-axis diameter) between dark and light regions, identifies the facets as (112) planes, which in a chalcopyrite are equivalent to (111) planes in a III–V zinc blende crystal.

For our application, the radial segregation described above is highly desirable, since the absorbing defects are zoned to the edges of the boule (material which is normally discarded) so that low-loss samples for nonlinear frequency conversion can be cut from the clear central region. In addition, this selective segregation offers a unique opportunity to compare the properties of samples with very high and very low defect concentrations in hopes of identifying and ultimately eliminating the responsible defects.

3. Defect characterization

IR spectrophotometry, electron paramagnetic resonance (EPR), trace analysis, and Hall effect measurements were used to characterize the “light” and “dark” regions of HGF-grown CdGeAs₂ crystals.

3.1. Absorption spectra

Room temperature absorption spectra were measured from 2.5 to 16 μm using a Perkin Elmer model 1420 ratio-recording infrared spectrophotometer. The results are shown in Fig. 4. Note the prominent mid-IR absorption peak at 5.5 μm in the dark region, which is 26 times higher than that in the light central core. This large difference is consistent with the very large differences in segregation coefficient that have been observed for growth on- and off-of a {111}-type facet. Kildal [11] suggested that this absorption peak was related to the presence of uncompensated native acceptors which are shallow enough ($E_a \sim 100$ meV) to be thermally ionized, leaving holes in the uppermost valence band and thereby allowing intra-band transitions from the two lower valence bands into the upper one. The 5.5-μm peak is due to transitions from the next lowest valence band, whereas the absorption tail near the band edge corresponds to transitions from the deeper valence band.

3.2. EPR measurements

EPR has been applied to CdGeAs₂ in an attempt to identify these native acceptors. A large EPR signal characteristic of a high concentration of acceptor-type defects has in fact been observed in CdGeAs₂, and measurements on the “light” and “dark” material described here showed that the magnitude of the signal scaled with the large difference in absorption coefficient between the two regions. Unfortunately the observed EPR lines are broad, fairly isotropic, and lack distinctive hyperfine structure indicative of the local defect environment.

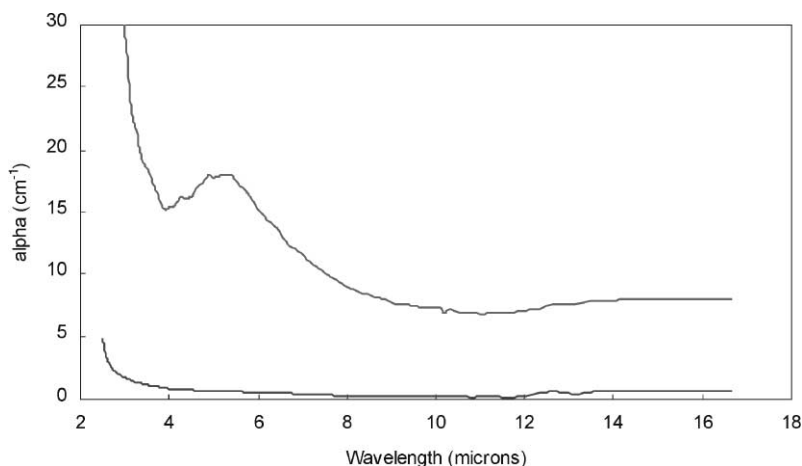


Fig. 4. Room temperature absorption spectra of light (lower curve) and dark (upper curve) regions of the HGF-grown CdGeAs_2 sample shown in Fig. 2a.

3.3. Trace analysis

Trace chemical analysis on CdGeAs_2 material cut from the dark and light regions was performed by glow discharge mass spectrometry (GDMS). The results are listed in Table 1. Although they indicate a slightly greater number of impurities in the “dark” region, the concentrations are very low and in most cases not much higher than observed in the light region. Note that none of the measured impurities that could act as acceptors are present in a concentration that could account for the observed optical absorption. This fact further supports the assertion that the acceptor defects are intrinsic (i.e., V_{Cd} , Ge_{As} , or Cd_{Ge}). No detectable differences in the stoichiometry of the matrix elements (Cd, Ge, As) could be found by EDAX measurements.

3.4. Hall effect analysis

The narrow band gap of CdGeAs_2 facilitates the use of electrical characterization techniques, and although Hall effect analysis can provide no direct information regarding the exact identity of the participating defects, it is particularly well suited to quantitative determination of defect concentrations and activation energies. Early measurements

Table 1
GDMS results on “light” and “dark” samples cut from an undoped boule of CdGeAs_2 . Concentrations are given in ppm, ... indicates the element is not present at the limit of detectability

Element	Concentration (ppm)	
	“Dark” region	“Light” region
Li	0.002	—
B	0.015	...
C	10	3
O	10	7
Na	0.01	...
Mg	0.003	...
Al	0.13	0.03
Si	0.04	...
P	0.33	0.32
S	0.34	0.065
Ti	0.02	...
Cr	0.025	...
Co	0.001	...
Ni	0.07	...
Cu	0.03	0.02
Zn	0.035	0.03
Se	0.62	0.37
Sb	0.003	...
Te	0.007	0.006
Pt	0.12	0.1

Table 2
Temperature-dependent Hall effect results on “light” and “dark” CdGeAs₂ samples

Sample	$p@300\text{ K}$ ($\times 10^{16}\text{ cm}^{-3}$)	$\mu(a\text{-axis})$ (cm^2/Vs)	$\mu(c\text{-axis})$ (cm^2/Vs)	Activation Energy (meV)	Compensation Ratio	N_a estimate (cm^{-3})
“Dark” CGA	3.1	124	446	109	0.25	$> 10^{18}$
“Light” CGA	0.089	155	620	125	0.95	$\sim 2.5 \times 10^{17}$

indicated that nearly all CdGeAs₂ samples are p-type, with acceptor activation energy between 100 and 350 meV. This discrepancy in activation energies was attributed to the presence of two different acceptors, with the deeper one (at 300 meV) being more common in most samples in the literature.

The results of temperature-dependent Hall measurements performed on “light” and “dark” CdGeAs₂ samples are listed in Table 2. Because of the anisotropic transport properties of CdGeAs₂, measurements in each case were made on matched sets of wafers fabricated with the *c*-axis perpendicular and parallel to the plane of the wafer, respectively, [12]. Firstly, note that the acceptor concentration was over an order of magnitude lower in the light material, which tracked the difference in absorption coefficient. (The 10^{18} value represents a lower limit for the dark material: the high acceptor concentration made the material so p-type that heating could not induce the p-to-n transition needed to accurately quantify the results.) Secondly, it is significant that the samples cut from the “dark” region of the crystal were only about 25% compensated, while those cut from the “light” region were 95% compensated. This compensation in both cases is due to the presence of native donor defects, as the boule was undoped. The high degree of compensation in the light region results in lower intra-band (5.5- μm) absorption, while the reduced acceptor concentration results in a weaker near-edge absorption tail. Finally, note that the average acceptor activation energy is higher in the light material than the dark material, indicating that the shallower acceptors are preferentially zoned to the dark region with respect to the deeper acceptors. These deeper

acceptors are less easily ionized at room temperature, resulting in less intra-band absorption.

Acknowledgements

The authors wish to thank Kevin Stevens, Larry Halliburton, and Nancy Giles at West Virginia University for the EPR results, and Mike Winn at Sanders for assistance with the LWIR imaging. This work was supported by the Air Force Research Laboratory Materials Directorate under contract number F33615-94-C-5415.

References

- [1] G.W. Iseler, H. Kildal, N. Menyuk, J. Electron. Mater. 7 (1978) 737.
- [2] R.S. Feigelson, R.K. Route, J. Crystal Growth 49 (1980) 261.
- [3] P.G. Schunemann, T.M. Pollak, U.S. Patent No. 5,611,856, March 18, 1997.
- [4] P.G. Schunemann, T.M. Pollak, J. Crystal Growth 174 (1997) 272.
- [5] P.G. Schunemann, T.M. Pollak, MRS Bull. 23 (1998) 23.
- [6] P.G. Schunemann, K.L. Schepler, P.A. Budni, MRS Bull. 23 (1998) 45.
- [7] K.L. Vodopyanov, P.G. Schunemann, Opt. Lett. 23 (1998) 1096.
- [8] S.C.H. Wang, G. Dudoff, S. Jost, J. Roussis, J. Voelker, M. Winn, T. Wyman, Proc. SPIE 2225 (1994) 335.
- [9] K.F. Hulme, J.B. Mullin, Philos. Mag. 4 (1959) 1286.
- [10] K. Morizane, A.F. Witt, H.C. Gatos, J. Electrochem. Soc. 115 (1968) 747.
- [11] H. Kildal, Phys. Rev. B 10 (1974) 5082.
- [12] A.J. Ptak, S. Jain, T.H. Myers, P.G. Schunemann, S.D. Setzler, T.M. Pollak, in: Infrared applications of semiconductors III, I. Ferguson, M.O. Manasreh, B.H. Stadler, Y.-H. Zhang (Eds.), Materials Research Society Symposium Proceedings, Vol. 607, Materials Research Society, Pittsburgh, 2000, pp. 427–432.